Contents lists available at ScienceDirect

Wave Motion

journal homepage: www.elsevier.com/locate/wamot

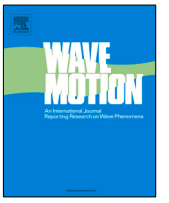

Highlights

Thermal effects in short laser pulses: Suppression of wave collapse

Wave Motion xxx (xxxx) xxx

Benjamin F. Akers*, Tony Liu

- A model for studying thermal effects on short laser pulses is proposed.
- The model includes a parameter measuring the importance of thermal and Kerr effects.
- The model is numerically simulated; evidence for wave collapse in this model is observed.
- Thermal effects increase the distance and amplitudes required to observe collapse.
- A diagram of the effect of the thermal parameter on wave collapse is constructed.

Please cite this article as: B.F. Akers and T. Liu, Thermal effects in short laser pulses: Suppression of wave collapse, Wave Motion (2022) 103079, https://doi.org/10.1016/j.wavemoti.2022.103079.

WAMOT: 103079

ARTICLE IN PRESS

Wave Motion xxx (xxxx) xxx

Contents lists available at ScienceDirect

Wave Motion

journal homepage: www.elsevier.com/locate/wamot

Thermal effects in short laser pulses: Suppression of wave collapse

Benjamin F. Akers [*,1], Tony Liu [1]

Department of Mathematics and Statistics, Air Force Institute of Technology, Dayton, OH, United States of America

ARTICLE INFO

Article history:
Received 14 March 2022
Received in revised form 12 July 2022
Accepted 21 September 2022
Available online xxxx

MSC:
35B35
76B15

Keywords:
Wave-collapse
Pulsed lasers
Schrödinger equation

ABSTRACT

An envelope model for short laser pulses is proposed. These pulses are short compared to fluid motion timescales and long compared to electron thermalization timescales. Numerical simulation of the thermal blooming of laser pulses at powers near the boundary of the self-focusing regime is presented in this model. The model includes terms representing the contributions of thermal blooming and the Kerr effect. In the context of the model, thermal blooming and the Kerr effect compete; Kerr driving and thermal blooming suppressing wave collapse. The dynamics of pulses whose energies are near the collapse threshold are numerically simulated.

Published by Elsevier B.V.

1. Introduction

Laser pulses have a variety of applications, including micromachining, ablation, surgery, tunneling, welding, remote sensing, and many more [1–5]. The large irradiance levels achievable in these pulses create a large number of nonlinear effects which are not observed in the continuous wave[2] case. These nonlinear effects include, but are not limited to plasma defocusing and absorption, multiphoton and avalanche ionization, and the Kerr effect [6,7]. The importance of these effects depends on the irradiance levels achieved, with the plasma and ionization effects becoming more important as irradiance increases [8]. In this work we focus on two nonlinear effects which require the smallest laser powers, often still quite large, to be relevant: the Kerr effect and thermal blooming.

Thermal blooming is the process wherein the laser heats its propagation medium (for example by molecular absorption [9,10]) and the resulting temperature fluctuations feedback on the beam via changes in refractive index. The result, sometimes referred to as thermal lensing [11], has a defocusing effect on the beam spot. In the presence of cross wind [12], or due to convection in a stagnation zone [13], thermal blooming can lead to crescent-shaped beam spots. There is a long history of studying thermal blooming in the continuous wave case [14–18]; it has also been simulated for pulsed lasers [6,19].

A standard technique for propagation studies of thermal blooming (at least when beam dynamics are simulated) is to use a paraxial approximation to the laser, resulting in a Schrödinger equation for the envelope of the electric field [20–22].

* Corresponding author.
E-mail addresses: Benjamin.Akers@afit.edu (B.F. Akers), Tony.Liu@afit.edu (T. Liu).

[1] Both authors contributed equally to all portions (numerics, modeling and analysis).

[2] Continuous wave (CW) lasers have a steady beam with constant power, the alternative being pulsed lasers which alternate between 'on' and 'off' at some fixed repetition rate.

https://doi.org/10.1016/j.wavemoti.2022.103079
0165-2125/Published by Elsevier B.V.

In the nonlinear regime, Schrödinger's equation can exhibit finite time singularity, or wave-collapse, depending on the relative signs of the linear and nonlinear terms (and the dimension) [23–26]. In the regime where wave collapse occurs, localized initial data either focuses to a point (collapse) or disperse across the domain, depending on a measure of the initial wave's energy. Mathematically, solitary wave solutions to the nonlinear Schrödinger equation have energies which lie exactly on this boundary [27,28]. In laser propagation, energies above this boundary correspond to beam irradiances which spontaneously filament at some distance from the aperture [29,30]. The addition of damping terms can suppress collapse [31,32] as can higher order dispersion [33]. In this work, a non-local nonlinear term due to heating is observed to suppress collapse.

The model proposed here considers the evolution of a continuous temperature field. This modeling assumption places an implicit restriction on the timescales for which the model is valid, the time has to be long enough for the notion of temperature to be well-defined [34]. Ultra short pulses can occur at pulse rates faster than the electron relaxation time, driving the fluid out of local thermal equilibrium [35,36]. In this circumstance it is common to introduce separate lattice and electron temperatures, and use a multi-physics approach to couple the laser with the molecular dynamics [37,38]. Although molecular dynamics will not be employed here, the continuum model should agree with the molecular dynamics in the limit.

In this work, the competing effects of thermal blooming and the Kerr effect on short laser pulses are considered in a simple model, valid in the regime where these two effects are of similar importance. The regime is one where the laser amplitude is near the threshold for self-focusing, referred to here as the boundary of wave collapse, but where the pulse rate is long enough to see thermal effects. In the context of this model, the boundary of wave collapse depends on the relative magnitude of the thermal blooming and Kerr effect, as one should expect, with thermal blooming acting to increase the amplitudes required to observe collapse-suppressing wave collapse at fixed amplitude. Numerical evolution of initial data of a variety of amplitudes are reported, focusing on the dependence of the solution dynamics, e.g. whether the waves collapse or disperse, as a function of the thermal blooming coefficient and the wave's initial amplitude. Thermal blooming is also observed to change the distance from the aperture and time of collapse for beams above the critical threshold.

2. Modeling short pulses with near-critical energy

In this work, short pulse lasers are modeled with an envelope equation

$$A_z + \frac{ik_0''}{2}A_{\tau\tau} + \frac{i}{2k_0 n_0}A_{xx} + (in_1 + \alpha)A = 0, \tag{2.1}$$

in which k_0'' is the Group Velocity Dispersion (GVD), n_1 are nonlinear corrections to the base refractive index n_0, α is the loss due to absorption, z is the propagation coordinate, x is a transverse spatial coordinate, and $\tau = t - z/v_g$ is the retarded time coordinate with v_g the group velocity [7]. We consider two nonlinear contributions to n_1, from thermal blooming and the Kerr effect [39], $n_1 = n_{1,T} + n_{1,K}$,

$$n_{1,T} = -\frac{k_0(n_0 - 1)(T - T_0)}{T_0}, \qquad n_{1,K} = \frac{k_0\eta_2}{\eta_0}|A|^2.$$

The thermal blooming term, $n_{1,T}$, assumes an ideal gas at a temperature T which has small fluctuation about an average temperature T_0; the Gladstone-Dale relationship to refractive index fluctuations to density fluctuations, as in [13]. In Eq. (2.1), we have neglected some physical effects in order to focus on the competition between thermal blooming and Kerr. These effects are important at larger laser energies, and include multiphoton absorption, electron plasma defocusing and absorption, and high-order Kerr effects [7,40,41]. Previous work making these modeling choices, neglecting higher order terms and using similar envelope equations, include [6,8]; this work is distinct from these in its simulation of the evolution of the temperature field.

Eq. (2.1) is a generalized nonlinear Schrödinger equation in 2+1 dimensions (two transverse and one propagation dimension). The character of such equations depends crucially on the relative signs of the linear and nonlinear terms, which dictate whether the equation is of focusing or defocusing type [23,42]. The sign of k_0'', the Group Velocity Dispersion, depends both on material and wavelength [43]. In this work, we will work in a scaled model where only the signs effect our analysis. Example of values of the GVD coefficient are $k_0'' = 360$ fs^2/cm in fused silica [39] or $k_0'' = 0.2$ fs^2/cm in air (both of these values are at a wavelength of $\lambda = 800$ nm) [41,44] (note that other signs of k_0'' are possible at other wavelengths in other propagation media [43,45]).

The temperature in (2.1) will be assumed to be initially constant, but permitted to evolve in time, by the equation

$$T_t + (u \cdot \nabla)T = \kappa \Delta T + \beta|A|^2, \tag{2.2}$$

in which κ is the thermal diffusivity and $\beta = \frac{\alpha}{c_p\rho}$ represents the heating due to absorption by the laser [13]. The parameter c_p is the specific heat, ρ is the density of the propagation medium.

2.1. Parameters and non-dimensionalization

Before combining (2.1) and (2.2) we note that the importance of the terms in these equations varies with scenario. To observe the relative sizes of each term in these equations we will non-dimensionalize the equations,

$$\tilde{T} = \frac{T - T_0}{T_1}, \qquad \tilde{A} = \frac{A}{A_0}, \qquad \tilde{\tau} = \frac{\tau}{\mathcal{T}}, \qquad \tilde{t} = \frac{t}{\mathcal{T}}, \qquad \tilde{\mathbf{x}} = \frac{\mathbf{x}}{L}, \qquad \tilde{\mathbf{u}} = \frac{\mathbf{u}}{U}$$

where L is a lengthscale, $\mathcal{T}$ is a timescale, T_1 is a scale for temperature fluctuations, T_0 is the undisturbed temperature, and A_0^2 is typical laser irradiance. After rescaling, and having dropped the tilde's on the independent variables, the coupled laser-temperature equations are

$$\tilde{T}_t + \frac{\mathcal{T}U}{L}\tilde{u}\cdot\nabla\tilde{T} = \frac{\kappa\mathcal{T}}{L^2}\Delta\tilde{T} + \frac{\beta A_0^2\mathcal{T}}{T_1}|\tilde{A}|^2 \tag{2.3}$$

$$\tilde{A}_z + \frac{ik_0''L}{2\mathcal{T}^2}\tilde{A}_{\tau\tau} + \frac{i}{2k_0L}\tilde{A}_{xx} - i\left(\frac{k_0(\eta_0-1)T_1\tilde{T}L}{T_0} - \frac{k_0\eta_2A_0^2L}{\eta_0}|\tilde{A}|^2 + \alpha L\right)\tilde{A} = 0 \tag{2.4}$$

Setting the temperature fluctuation scale based on the heating term, $T_1 = \beta A_0^2\mathcal{T}$, the temperature equation becomes

$$\tilde{T}_t + \epsilon_1\tilde{u}\cdot\nabla\tilde{T} = \epsilon_2\Delta\tilde{T} + |\tilde{A}|^2 \tag{2.5}$$

The parameters ϵ_j are small when the timescale of the pulse is small compared to the diffusive and convective timescales,

$$\frac{\mathcal{T}U}{L} \ll 1 \qquad \text{and} \qquad \frac{\mathcal{T}\kappa}{L^2} \ll 1. \tag{2.6}$$

Neglecting the ϵ_j terms in (2.5), then changing variables from t to $\tau = t - \frac{z}{v_g}$ gives[3]

$$\tilde{T}_\tau = |\tilde{A}|^2. \tag{2.7}$$

Eqs. (2.6) restricts from above the timescale for which model (2.7) can be used. Since this is an equation for the continuous temperature field (as opposed to lattice or phonon temperatures [34,36,38,46]), the pulse timescale is also implicitly restricted from below. In order for the lattice and phonon temperatures to equilibrate, timescales should be larger than 10^{-11} s in fused silica [47] or 10^{-9} s in air [37] (the latter number depending on moisture content [35]). As a result, this model should be considered in the intermediate regime, pulses which are fast relative to fluid motion and diffusion, but slow compared to electron energy transitions and thermalization. The timescales for which (2.7) is valid depend on the medium, two examples are below

Material	U	κ	L	Timescales
Fused silica	0	0.0138 cm^2/s	1 cm	$10^{-11}\text{s} \ll \mathcal{T} \ll 10^2\text{s}$
Air	10 cm/s	0.2 cm^2/s	1 cm	$10^{-9}\text{s} \ll \mathcal{T} \ll 10^{-1}\text{s}$

For continuous wave (CW) studies, the solution to the temperature Eq. (2.7) is sometimes approximated as a power series, e.g. $\tilde{T} = \tau|\tilde{A}|^2 + O(\tau^2)$ [48]. Such an expansion does not make sense for pulse lasers, where the temporal oscillations are of fundamental interest. Instead, the differential equation for the temperature equation is kept as (2.7), and coupled to the envelope equation,

$$\tilde{A}_z + i\lambda_1\tilde{A}_{\tau\tau} + i\lambda_2\tilde{A}_{xx} - i\left(\delta\tilde{T} - \chi|\tilde{A}|^2 + \tilde{\alpha}\right)\tilde{A} = 0 \tag{2.8}$$

All of the coefficients in (2.8) can be small depending on the physical scenario. In this work we will consider the case where $\tilde{\alpha}$ and δ are small. The former will be neglected (a study of the effect linear damping on collapse can be found in [32]); the latter will be used to measure the relative importance the thermal blooming term compared to the Kerr nonlinearity.

2.2. Wave collapse

For simplicity of presentation and analysis, system (2.7) & (2.4) is rescaled to

$$A_z + iA_{\tau\tau} + iA_{XX} - i(\delta T - |A|^2)A = 0 \tag{2.9a}$$

$$T_\tau = |A|^2 \tag{2.9b}$$

[3] This change of variables can also be done before neglecting the spatial derivatives in (2.5), in which case the change of variables introduces a few new terms, each of which have smaller coefficients than those neglected between (2.5) and (2.7).

The remaining non-unitary coefficient, δ, measures the relative importance of the thermal effects (defocusing) to the Kerr effect (focusing). This model is novel to this work, and should not be confused with other generalized nonlinear Schrödinger equations, the most similar being the Davey–Stewartson [42,49] and Schrödinger–Debye systems [26,50].

When $\delta = 0$, (2.9) decouples and (2.9a) is a focusing nonlinear Schrödinger equation which is known to exhibit a finite time singularity, known as wave collapse. A classic argument [23,42,51,52] shows that the solutions to Eq. (2.9a) (with $\delta = 0$) whose initial data are above a certain amplitude threshold localize to a point. We present this argument below.

Eq. (2.9a) (with $\delta = 0$) has two conserved quantities,[4]

$$M = \iint |A|^2 d\tau dx, \qquad \text{and} \qquad E = \iint |\nabla A|^2 - \frac{1}{2}|A|^4 \, d\tau dx.$$

With the knowledge that M and E are constant in the evolution of (2.9) (with $\delta = 0$), collapse is predicted by the evolution of the quantity

$$P(z) = \iint (x^2 + \tau^2)|A|^2 \, d\tau dx. \tag{2.10}$$

It is a straightforward, though tedious, exercise to show that P satisfies the equation[5]

$$\frac{d^2P}{dz^2} = 8E. \tag{2.11}$$

Since E is constant in solutions of Eq. (2.9a) (with $\delta = 0$), the differential Eq. (2.11) is trivial to solve, supporting parabolic trajectories. These parabolic trajectories reach $P = 0$ at finite z whenever $E < 0$. At this value of z the intensity $|A|$ must be wholly concentrated at the origin - a phenomenon called wave collapse. Brief examination of E reveals that this happens for any initial profile shape of sufficient amplitude (since the negative term in E is proportionate to a higher power of the amplitude than the positive term). Thus for each fixed beam profile, there will be an amplitude threshold for which the wave collapses. Below this threshold, waves disperse. Solitary wave profiles live balanced at $E = 0$ and neither disperse nor collapse [56]. For the numerical investigations in this work, we use a spatial and temporally localized pulse of the form

$$A(x, \tau, 0) = A_0 \operatorname{sech}\left(\frac{1}{4}x\right) \operatorname{sech}\left(\frac{1}{4}\tau\right). \tag{2.12}$$

In the next section we observe, numerically, the effect of $\delta \neq 0$ in model (2.9) with particular attention paid to the localization and growth of solutions near the collapse threshold.

3. Numerical simulations

The numerical simulations in this work use a Fourier-split step scheme, as has become the industry standard for simulations of laser-envelope equations [21,57,58]. This method splits Eq. (2.9) into

$$A_z + iA_{\tau\tau} + iA_{XX} = 0 \tag{3.1}$$

and

$$A_z - i(\delta T - |A|^2)A = 0, \tag{3.2a}$$

$$T_\tau = |A|^2. \tag{3.2b}$$

After splitting, (3.1) is integrated in Fourier space with no time discretization errors. For system (3.2), at each z-step (3.2b) is integrated using the trapezoid scheme. To integrate (3.2a), given T from (3.2b), notice that (3.2a) conserves $|A|^2$,

$$A_z = i(\delta T - |A|^2)A, \qquad \bar{A}_z = -i(\delta T - |A|^2)\bar{A}$$

which implies

$$|A|^2_z = A_z\bar{A} + \bar{A}_z A = i(\delta T - |A|^2)|A|^2 - i(\delta T - |A|^2)|A|^2 = 0.$$

Since $|A|^2$ is constant in z, one can exactly integrate (3.2a) (given the results from integrating Eq. (3.2b)). The combined scheme for (2.9) is spectrally accurate in x and second order in τ and z (due to the second order Strang splitting and trapezoid rule used to solve (3.2b)).

System (2.9) was simulated with a variety of initial amplitudes A_0 in (2.12) and thermal coefficients δ, on both sides of the collapse threshold. A depiction of a dispersing trajectory, below the collapse threshold, is in Fig. 2.1; a collapsing trajectory is depicted in Fig. 2.2. In the dispersing trajectory, Fig. 2.1, the solution's maximum monotonically decreases as it propagates in z. The profile also spreads out, becoming less focused as it evolves. In the collapsing trajectory,

[4] 'Conserved quantities' are those which are invariant in the evolution, see [53–55].

[5] This argument generalizes to higher dimensions, with small changes to Eq. (2.11).

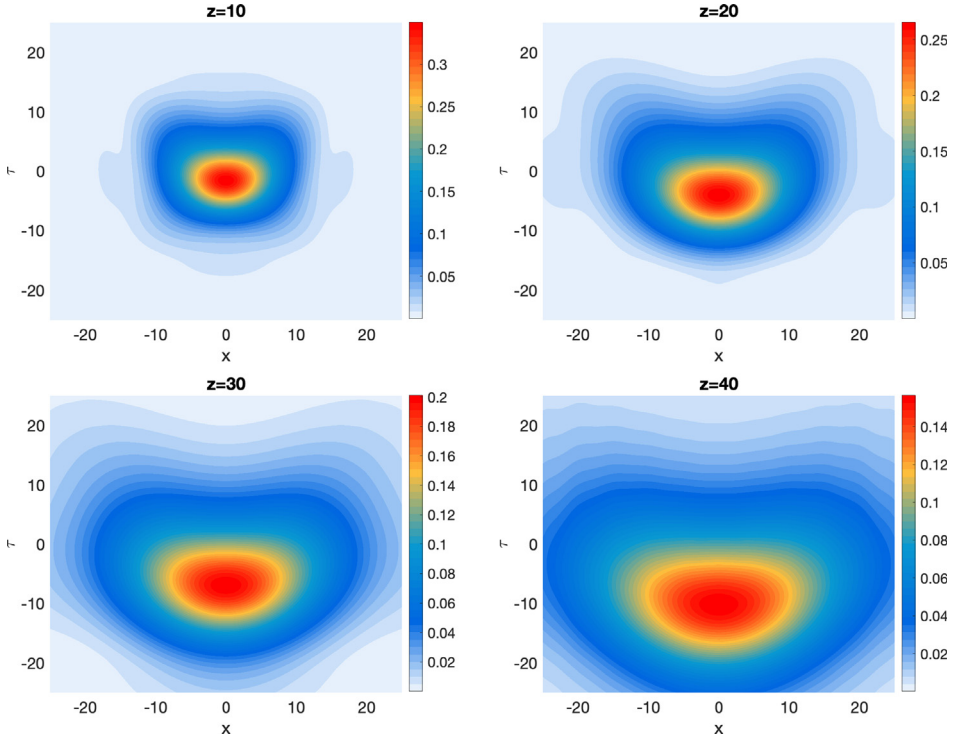

Fig. 2.1. The evolution of (2.12) with $A_0 = 0.4$ and $\delta = 0.1$ is depicted at a sampling of distances. This initial data has $E > 0$, thus is below the unperturbed ($\delta = 0$) collapse threshold. The evolution decays in amplitude and spreads out. Only a portion of the computational domain is shown.

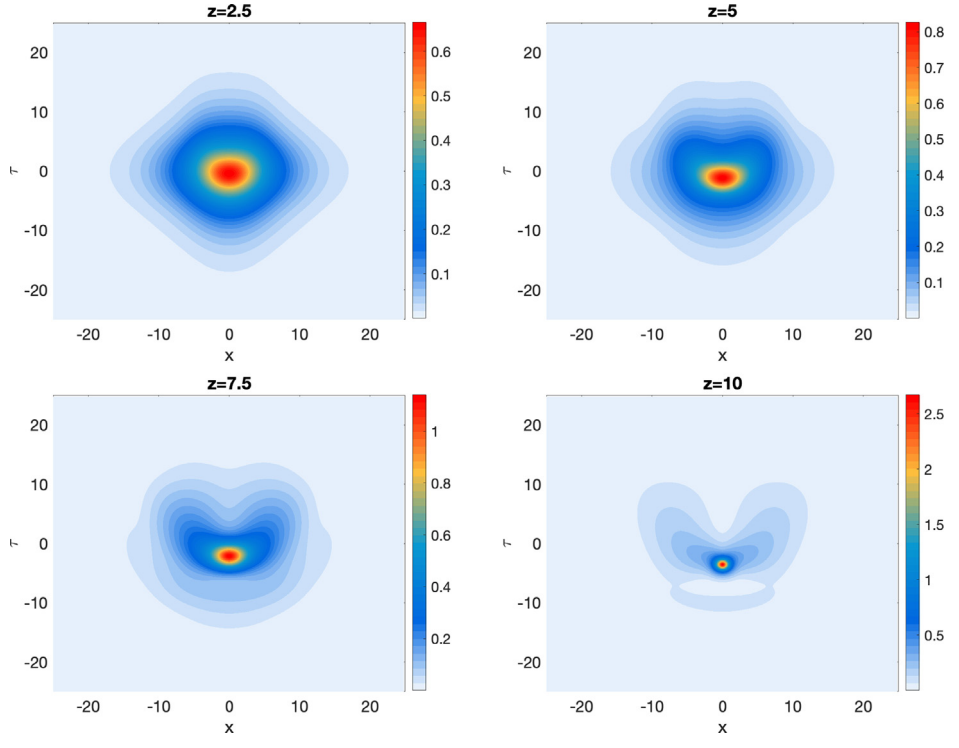

Fig. 2.2. The evolution of (2.12) with $A_0 = 0.6$ and $\delta = 0.1$ is depicted at a sampling of distances. This initial data has $E < 0$, thus is above the unperturbed ($\delta = 0$) collapse threshold. The evolution grows in amplitude and becomes increasingly localized. The entire computational domain is shown.

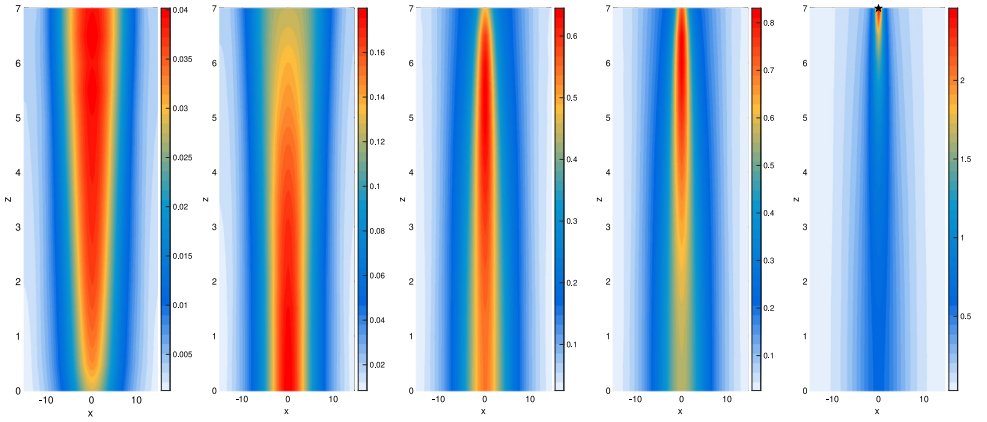

Fig. 3.1. Plots of the $|A|$ at a sequence of times in the x–z plane are depicted, for the initial data (2.12) with $A_0 = 0.6$ and $\delta = 0$. The sample times are, from left to right $\tau = -15, -7.5, -1.875, -1.41$ and 0. In this coordinate system $\tau = -15$ is when pulse is turned on; $\tau = 0$ is when the pulse has its peak amplitude at the aperture, $z = 0$. In this simulation, collapse occurs at $t = 0$, $z \approx 7.13$, marked with a star at the top of the right panel, at exactly the time when the peak amplitude leaves the aperture and at a shorter distance than when $\delta \neq 0$ (compare to Fig. 3.2).

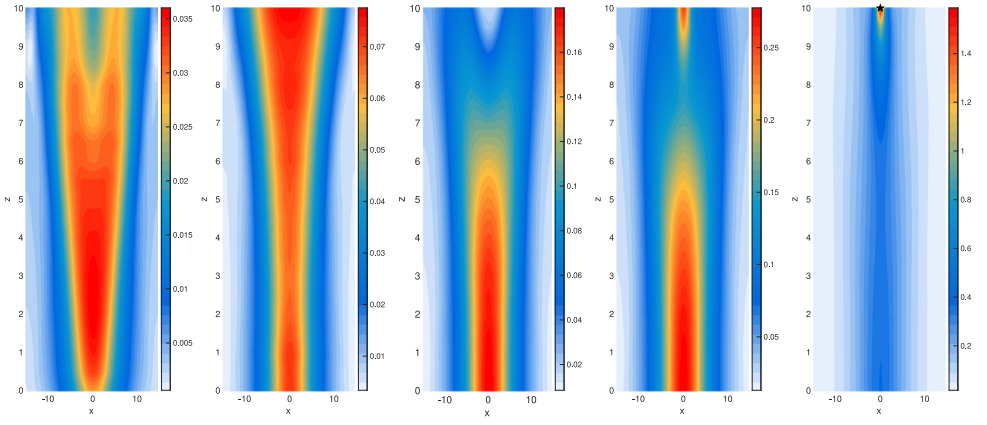

Fig. 3.2. Plots of the $|A|$ at a sequence of times in the x–z plane are depicted, for the initial data (2.12) with A_0 and $\delta = 0.1$. The sample times are, from left to right $\tau = -15, -11.25, -7.5, -5.625$, and -4.218. In this coordinate system $\tau = -15$ is when pulse is turned on; $\tau = 0$ is when the pulse has its peak amplitude at the aperture, $z = 0$. In this simulation, collapse occurs at $t \approx -4.218$, $z \approx 10.12$, marked with a star at the top of the right panel, both earlier in time and further in distance than the same amplitude with $\delta = 0$ (see Fig. 3.1).

Fig. 2.2, the amplitude monotonically increases as the profile focuses. Although the numerical simulations cannot observe the trajectory all the way to collapse (the solution is ultimately too focused for any fixed grid spacing), the numerical observations include similar focusing dynamics as the $\delta = 0$ case (in terms of solution growth and localization), where collapse is known. A marked difference between the $\delta \neq 0$ and $\delta = 0$ settings is that the solution becomes crescent shaped in the $x\tau$-plane. This crescent is reminiscent of, but should not be confused with, the classic thermal blooming crescent, which occurs in space rather than space–time. The authors have, to date, resisted the temptation to make an analogy regarding a 'wind' in space–time.

In Figs. 2.1 and 2.2 solutions are plotted in the $x\tau$-plane, the natural one for reporting solutions of (2.9) as an evolution equation in z. It is more physical to report the solutions in the xz-plane at a sequence of τ. Two collapsing trajectories are depicted this way in Figs. 3.1 and 3.2. In these two figures one may observe the effect of $\delta \neq 0$ on collapse for initial amplitudes A_0 above the collapse threshold. The most noticeable difference between these two figures (which use the same initial amplitude $A_0 = 0.6$) is the distance that the pulse propagates in z before collapse. With $\delta = 0$, collapse occurs at $z \approx 7.13$; with $\delta = 0.1$ collapse occurs at $z \approx 10.12$. The thermal effects thus allow the beam to propagate $\approx 40\%$ farther before collapsing. The inclusion of thermal effects causes the collapse threshold to increase in amplitude and the collapse distance to increase in z. Both of these are thermally induced suppressions of collapse. Interestingly, the collapse location in space time is also shifted in τ by the presence of δ in the negative direction (see Fig. 2.2). Thus collapse happens earlier in be the presence of δ, and thermal effects could be said to enhance, rather than suppress, collapse as a function of τ.

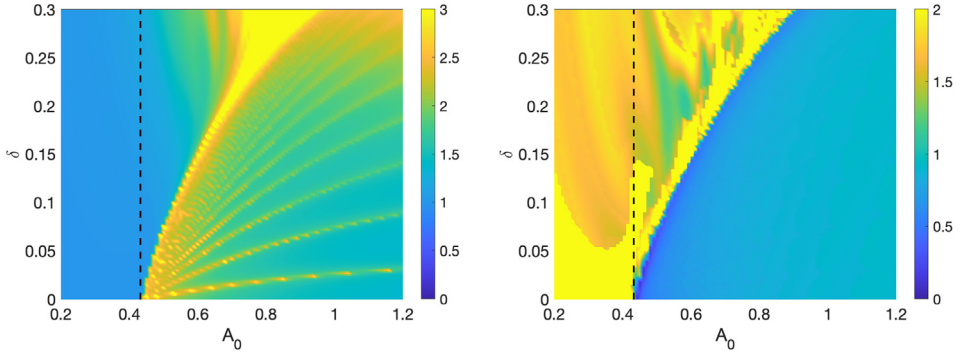

Fig. 3.3. Eq. (2.9) was simulated with a variety of δ and A_0 values for $z \in (0, 75]$ (simulations which collapse are stopped early). The threshold for wave collapse with $\delta = 0$ is marked with the vertical dashed line. **Left:** The value of the H_1 norm at the end of the simulation (normalized by the H_1 norm of the initial data). The H_1 norm is infinity at wave collapse, but may also grow for non-localized solutions. **Right:** The value of $\tilde{P}(z)$ at the end of the simulation, normalized by $\tilde{P}(0)$, If this ratio is less than one the solution is becoming more localized.

For system (2.9), with $\delta \neq 0$, the quantity E is not conserved and the ODE (2.11) is no longer satisfied. As alternative indicators of collapse, two solution metrics are tracked. These are the H_1 norm of the solutions,

$$\|A\|_{H_1} = \left(\iint |A_x|^2 + |A_\tau|^2 + |A|^2 \, dx \, d\tau \right)^{1/2}$$

and a modified version of the integral in (2.10),

$$\tilde{P} = \iint \left((\tau - \tau_m)^2 + x^2 \right) |A|^2 \, dx \, d\tau .$$

The quantity $\tilde{P}$ is a temporally shifted version the integral in (2.10). The shift τ_m is the location in time where the solution attains it maximal modulus over the entire simulation duration. For dispersing waves this time is $\tau_m = 0$; for collapsing waves this time is observed to be negative (and more negative the closer to the collapse threshold the initial data is). The H_1 norm and the seminorm P were computed for a variety of initial amplitudes, A_0, and coefficients, δ. With each pair, the initial data (2.12) was evolved either to $z = 75$ or until the solution became too localized for the grid spacing. The latter was measured by enforcing a threshold of 10^{-5} for the amplitude of the highest frequency Fourier modes. The results of these simulations are reported in Fig. 3.3.

Both panels of Fig. 3.3 give approximations of the boundary of wave collapse in parameter space. Wave collapse occurs when the solution both grows to infinity and localizing to a point. The growth is measured by the H_1 norm in the left panel, the localization is measured by $\tilde{P}$ in the right panel. The precise location of this boundary in parameter space is difficulty to interrogate, as the distance at which collapse occurs approaches infinity as one approaches the boundary. The simulation distance, $z = 75$, was chosen so that increasing the distance does not change Fig. 3.3 at the resolution at which it is reported.

4. Conclusion

Simulations of the effect of thermal blooming on wave collapse in short laser pulses were conducted. These simulations use an envelope model coupled with an equation for the temperature of the propagation medium. In the context of this model, temperature effects were seen to increase the distance at which wave collapse occurs, as well as increase the amplitude threshold at which collapse occurs, suppressing wave collapse. Solution dynamics were observed and phase diagrams of parameter space were created.

Declaration of competing interest

The authors declare the following financial interests/personal relationships which may be considered as potential competing interests: Benjamin Akers reports financial support was provided by Air Force Institute of Technology. Tony Liu reports financial support was provided by Air Force Institute of Technology. Benjamin Akers reports a relationship with Air Force Office of Scientific Research that includes: funding grants. Benjamin Akers reports a relationship with Office of Naval Research that includes: funding grants.

Acknowledgments

The authors would like to thank Steven Fiorino for useful discussions. B.F. Akers acknowledges support from the Air Force Office of Sponsored Research's Computational Mathematics Program via the project *Radial Basis Functions for Numerical Simulation* and the Office of Naval Research as part of the AIM-APL program. T. Liu acknowledges support from DEJEDI.

References

[1] X. Liu, D. Du, G. Mourou, Laser ablation and micromachining with ultrashort laser pulses, IEEE J. Quantum Electron. 33 (10) (1997) 1706–1716.
[2] P Rairoux, H Schillinger, S Niedermeier, M Rodriguez, F Ronneberger, R Sauerbrey, B Stein, D Waite, C Wedekind, H Wille, et al., Remote sensing of the atmosphere using ultrashort laser pulses, Appl. Phys. B 71 (4) (2000) 573–580.
[3] Holger Lubatschowski, G Maatz, A Heisterkamp, U Hetzel, W Drommer, H Welling, W Ertmer, Application of ultrashort laser pulses for intrastromal refractive surgery, Graefe's Arch. Clin. Exp. Ophthalmol. 238 (1) (2000) 33–39.
[4] Kristian Cvecek, Sarah Dehmel, Isamu Miyamoto, Michael Schmidt, A review on glass welding by ultra-short laser pulses, Int. J. Extrem. Manuf. 1 (4) (2019) 042001.
[5] Andrew Lawrence, Benjamin F. Akers, Propagation of high energy lasers through clouds: modeling and simulation, Appl. Opt. 59 (33) (2020) 10207–10216.
[6] Mark J. Schmitt, Mitigation of thermal blooming and diffraction effects with high-power laser beams, J. Opt. Soc. Amer. B 20 (4) (2003) 719–724.
[7] L. Bergé, A. Couairon, Nonlinear propagation of self-guided ultra-short pulses in ionized gases, Phys. Plasmas 7 (1) (2000) 210–230.
[8] Stellios Tzortzakis, Luc Bergé, Arnaud Couairon, Michel Franco, Bernard Prade, André Mysyrowicz, Breakup and fusion of self-guided femtosecond light pulses in air, Phys. Rev. Lett. 86 (24) (2001) 5470.
[9] Mark F Spencer, Salvatore J Cusumano, Jason D Schmidt, Steven T Fiorino, Impact of spatial resolution on thermal blooming phase compensation instability, in: Advanced Wavefront Control: Methods, Devices, and Applications VIII. Vol. 7816, International Society for Optics and Photonics, 2010, 781609.
[10] A.J. Glass, Thermal blooming in gases, Opto-Electron. 1 (4) (1969) 174–178.
[11] Walter Koechner, Thermal lensing in a Nd: YAG laser rod, Appl. Opt. 9 (11) (1970) 2548–2553.
[12] Jonathan Gustafsson, Benjamin F Akers, Jonah A Reeger, Sivaguru S Sritharan, Atmospheric propagation of high energy lasers: Thermal blooming simulation, Eng. Math. Lett. (2019).
[13] Benjamin F. Akers, Jonah A. Reeger, Numerical simulation of thermal blooming with laser-induced convection, J. Electromagn. Waves Appl. 33 (1) (2019) 96–106.
[14] Frederick G. Gebhardt, Twenty-five years of thermal blooming: an overview, in: Propagation of High-Energy Laser Beams Through the Earth's Atmosphere. Vol. 1221, International Society for Optics and Photonics, 1990, pp. 2–25.
[15] C.H. Chan, Effective absorption for thermal blooming due to aerosols, Appl. Phys. Lett. 26 (11) (1975) 628–630.
[16] John N. Hayes, Thermal blooming of laser beams in fluids, Appl. Opt. 11 (2) (1972) 455–461.
[17] Mark F. Spencer, Wave-optics investigation of turbulence thermal blooming interaction: II. Using time-dependent simulations, Opt. Eng. 59 (8) (2020) 081805.
[18] Noah R. Van Zandt, Steven T. Fiorino, Kevin J. Keefer, Enhanced, fast-running scaling law model of thermal blooming and turbulence effects on high energy laser propagation, Opt. Express 21 (12) (2013) 14789–14798.
[19] P Sprangle, JR Peñano, A Ting, B Hafizi, DF Gordon, Propagation of short, high-Intensity laser pulses in air, J. Dir. Energy 1 (2003) 73–92.
[20] A.P. Kiselev, Localized light waves: Paraxial and exact solutions of the wave equation (a review), Opt. Spectrosc. 102 (4) (2007) 603–622.
[21] Yuqiu Zhang, Xiaoling Ji, Xiaoqing Li, Hong Yu, Thermal blooming effect of laser beams propagating through seawater, Opt. Express 25 (6) (2017) 5861–5875.
[22] J Peñano, JP Palastro, B Hafizi, MH Helle, GP DiComo, Self-channeling of high-power laser pulses through strong atmospheric turbulence, Phys. Rev. A 96 (1) (2017) 013829.
[23] Catherine Sulem, Pierre-Louis Sulem, The Nonlinear Schrödinger Equation: Self-Focusing and Wave Collapse, Vol. 139, Springer Science & Business Media, 2007.
[24] Luc Bergé, Wave collapse in physics: principles and applications to light and plasma waves, Phys. Rep. 303 (5–6) (1998) 259–370.
[25] K.D. Moll, Alexander L. Gaeta, Gadi Fibich, Self-similar optical wave collapse: observation of the Townes profile, Phys. Rev. Lett. 90 (20) (2003) 203902.
[26] Gadi Fibich, George Papanicolaou, Self-focusing in the perturbed and unperturbed nonlinear Schrödinger equation in critical dimension, SIAM J. Appl. Math. 60 (1) (1999) 183–240.
[27] Benjamin Akers, Paul A. Milewski, Dynamics of three-dimensional gravity-capillary solitary waves in deep water, SIAM J. Appl. Math. 70 (7) (2010) 2390–2408.
[28] E.A. Kuznetsov, J. Juul Rasmussen, K. Rypdal, S.K. Turitsyn, Sharper criteria for the wave collapse, Physica D 87 (1–4) (1995) 273–284.
[29] G.G. Luther, J.V. Moloney, A.C. Newell, E.M. Wright, Self-focusing threshold in normally dispersive media, Opt. Lett. 19 (12) (1994) 862–864.
[30] Pavel Polynkin, Miroslav Kolesik, Critical power for self-focusing in the case of ultrashort laser pulses, Phys. Rev. A 87 (5) (2013) 053829.
[31] Boaz Ilan, Gadi Fibich, Semyon Tsynkov, Backscattering and nonparaxiality arrest collapse of damped nonlinear waves, SIAM J. Appl. Math. 63 (5) (2003) 1718–1736.
[32] Gadi Fibich, Self-focusing in the damped nonlinear Schrödinger equation, SIAM J. Appl. Math. 61 (5) (2001) 1680–1705.
[33] Boaz Ilan, Gadi Fibich, George Papanicolaou, Self-focusing with fourth-order dispersion, SIAM J. Appl. Math. 62 (4) (2002) 1437–1462.
[34] Janice M Hicks, Lynn E Urbach, E Ward Plummer, Hai-Lung Dai, Can pulsed laser excitation of surfaces be described by a thermal model? Phys. Rev. Lett. 61 (22) (1988) 2588.

[35] John M. Warman, Mei Zhou-lei, Dick van Lith, Electron thermalization in nanosecond pulse-ionized dry and humid air, J. Chem. Phys. 81 (9) (1984) 3908–3914.
[36] B. Rethfeld, A. Kaiser, M. Vicanek, G. Simon, Ultrafast dynamics of nonequilibrium electrons in metals under femtosecond laser irradiation, Phys. Rev. B 65 (21) (2002) 214303.
[37] Elise N. Pusateri, Heidi E. Morris, Eric M. Nelson, Wei Ji, Determination of equilibrium electron temperature and times using an electron swarm model with BOLSIG+ calculated collision frequencies and rate coefficients, J. Geophys. Res.: Atmos. 120 (15) (2015) 7300–7315.
[38] Xinwei Wang, Xianfan Xu, Molecular dynamics simulation of thermal and thermomechanical phenomena in picosecond laser material interaction, Int. J. Heat Mass Transfer 46 (1) (2003) 45–53.
[39] Scott A Diddams, Hilary K Eaton, Alex A Zozulya, Tracy S Clement, Characterizing the nonlinear propagation of femtosecond pulses in bulk media, IEEE J. Sel. Top. Quantum Electron. 4 (2) (1998) 306–316.
[40] Alexander L. Gaeta, Catastrophic collapse of ultrashort pulses, Phys. Rev. Lett. 84 (16) (2000) 3582.
[41] Le Wang, Cunliang Ma, Xiexing Qi, Wenbin Lin, The impact of the retarded Kerr effect on the laser pulses' propagation in air, Eur. Phys. J. D 69 (3) (2015) 1–5.
[42] GC Papanicolaou, Catherine Sulem, Pierre Louis Sulem, Xiao Ping Wang, The focusing singularity of the Davey-Stewartson equations for gravity-capillary surface waves, Physica D 72 (1–2) (1994) 61–86.
[43] Bob Proctor, Erik Westwig, Frank Wise, Characterization of a Kerr-lens mode-locked Ti: sapphire laser with positive group-velocity dispersion, Opt. Lett. 18 (19) (1993) 1654–1656.
[44] Arnaud Couairon, Michel Franco, Grégoire Méchain, Thomas Olivier, Bernard Prade, André Mysyrowicz, Femtosecond filamentation in air at low pressures: Part I: Theory and numerical simulations, Opt. Commun. 259 (1) (2006) 265–273.
[45] AV Mitrofanov, AA Voronin, MV Rozhko, DA Sidorov-Biryukov, AB Fedotov, A Pugžlys, V Shumakova, S Ališauskas, A Baltuška, AM Zheltikov, Self-compression of high-peak-power mid-infrared pulses in anomalously dispersive air, Optica 4 (11) (2017) 1405–1408.
[46] Katherine C Phillips, Hemi H Gandhi, Eric Mazur, SK Sundaram, Ultrafast laser processing of materials: a review, Adv. Opt. Photonics 7 (4) (2015) 684–712.
[47] G.L. Eesley, Generation of nonequilibrium electron and lattice temperatures in copper by picosecond laser pulses, Phys. Rev. B 33 (4) (1986) 2144.
[48] David C. Smith, High-power laser propagation: thermal blooming, Proc. IEEE 65 (12) (1977) 1679–1714.
[49] A. Davey, Keith Stewartson, On three-dimensional packets of surface waves, Proc. R. Soc. Lond. Ser. A Math. Phys. Eng. Sci. 338 (1613) (1974) 101–110.
[50] Adán J. Corcho, Jorge Drumond Silva, On the unboundedness of higher regularity Sobolev norms of solutions for the critical Schrödinger–Debye system with vanishing relaxation delay, Nonlinearity 30 (1) (2016) 300.
[51] J. Juul Rasmussen, K. Rypdal, Blow-up in nonlinear Schrödinger equations-I A general review, Phys. Scr. 33 (6) (1986) 481.
[52] Vladimir E. Zakharov, Collapse of langmuir waves, Sov. Phys.—JETP 35 (5) (1972) 908–914.
[53] Randall J. LeVeque, Randall J. Leveque, Numerical Methods for Conservation Laws, Vol. 214, Springer, 1992.
[54] Peter D. Lax, Periodic solutions of the KdV equation, Comm. Pure Appl. Math. 28 (1) (1975) 141–188.
[55] Harvey Segur, Mark J. Ablowitz, Asymptotic solutions and conservation laws for the nonlinear Schrödinger equation. I, J. Math. Phys. 17 (5) (1976) 710–713.
[56] Benjamin Akers, Paul A. Milewski, A model equation for wavepacket solitary waves arising from capillary-gravity flows, Stud. Appl. Math. 122 (3) (2009) 249–274.
[57] Oleg V Sinkin, Ronald Holzlöhner, John Zweck, Curtis R Menyuk, Optimization of the split-step Fourier method in modeling optical-fiber communications systems, J. Lightwave Technol. 21 (1) (2003) 61.
[58] Shaokang Wang, Andrew Docherty, Brian S Marks, Curtis R Menyuk, Comparison of numerical methods for modeling laser mode locking with saturable gain, J. Opt. Soc. Amer. B 30 (11) (2013) 3064–3074.